Proton Affinity Ladders from Variable-Temperature Equilibrium Measurements. 1. A Reevaluation of the Upper Proton Affinity Range

ARTICLE *in* JOURNAL OF THE AMERICAN CHEMICAL SOCIETY · JUNE 1991

Impact Factor: 12.11 · DOI: 10.1021/ja00012a012

2 AUTHORS, INCLUDING:

Michael Noah Mautner
Virginia Commonwealth University
205 PUBLICATIONS **5,429** CITATIONS

surfaces eventually present binding sites for the anionic S donors, but the precise nature of such sites is not clear. Future studies are to be directed toward studies of other crystal orientations to establish the scope and origins of selective binding, but it is clear that freshly etched (0001) CdX shows strong adsorption of MoS_4^{2-} and $Et_2NCS_2^-$ on the Cd-rich face which yields a very large effect on E_{FB}.

Considering the high degree of non-uniform binding of MoS_4^{2-} on the etched Cd-rich face of CdSe, we intend to investigate the distribution of adsorbates or reactants in other instances, including CdS,[24] GaAs,[25-27] and InP,[28] where surface modification yields physical and chemical changes or significant improvements in photoelectrochemical cells. Our data show that the AES technique is useful in detecting ~1 monolayer converages at a lateral resolution of <1 μm on the semiconductor surfaces. We have previously demonstrated AES to be useful for mapping surface composition of Au or Pt microelectrodes on Si_3N_4 substrates at <1-μm resolution for molecular monolayers.[29] For the modified semiconductor surfaces an aim is to relate non-uniform coverage of adsorbates with electrochemical behavior. For example, our observations are consistent with frequency-dependent interfacial capacitance measurements[30] which have been interpreted to mean that the Cd face of (0001) CdS is composed of regions with different values of E_{FB}.

A final point of interest concerns the magnitude of E_{FB} shifts for CdS and CdSe for MoS_4^{2-} vs $Et_2NCS_2^-$.[1] We find that the MoS_4^{2-} results in a larger shift on the Cd-rich face of CdSe (0.7–0.9 V) than on CdS (0.4–0.6 V) whereas it has been found[1] that $Et_2NCS_2^-$ yields a similar shift (~1 V) on CdS and CdSe. These differences, albeit modest in some ways, suggest that very subtle structural factors govern the coordination of the anionic S donors on CdX. The more highly charged MoS_4^{2-} does not lead to a larger shift in E_{FB} than found for $Et_2NCS_2^-$; in fact, the shift is somewhat smaller! A systematic study of $R_2NCS_2^-$ derivatives if planned, in order to establish steric and electronic effects on the binding of the dithiocarbamates to CdX.

Acknowledgment. We thank the United States Department of Energy, Office of Basic Energy Sciences, Division of Chemical Sciences for support of this research. We acknowledge use of XPS and Auger facilities acquired through the joint Harvard/M.I.T. University Research Initiative funded by the Defense Advanced Research Projects Agency.

Registry No. CdS, 1306-23-6; CdSe, 1306-24-7; MoS_4^{2-}, 16330-92-0; $Et_2NCS_2^-$, 147-84-2; HCl, 7647-01-0; $[Et_4N]_2MoS_4$, 14348-09-5; Na-$[Et_2NCS_2]$, 148-18-5.

(24) (a) Meyer, G. J.; Leung, L. K.; Yu, J. C.; Lisensky, G. C.; Ellis, A. B. *J. Am. Chem. Soc.* **1989**, *111*, 5146. (b) Campbell, B. D.; Farnsworth, H. E. *Surf. Sci.* **1968**, *10*, 197.

(25) Parkinson, B. A.; Heller, A.; Miller, B. *Appl. Phys. Lett.* **1978**, *33*, 521.

(26) Abrahams, I. L.; Tufts, B. J.; Lewis, N. S. *J. Am. Chem. Soc.* **1987**, *109*, 3472.

(27) Tufts, B. J.; Abrahams, I. L.; Santangelo, P. G.; Ryba, G. N.; Casagrande, L. G.; Lewis, N. S. *Nature* **1987**, *326*, 861.

(28) Spool, A. M.; Daube, K. A.; Mallouk, T. E.; Belmont, J. A.; Wrighton, M. S. *J. Am. Chem. Soc.* **1986**, *108*, 3155.

(29) (a) Hickman, J. J.; Zou, C.; Ofer, D.; Harvey, P. D.; Wrighton, M. S.; Laibinis, P. D.; Bain, C. D.; Whitesides, G. M. *J. Am. Chem. Soc.* **1989**, *111*, 7271. (b) Laibinis, P. D.; Hickman, J. J.; Wrighton, M. S.; Whitesides, G. M. *Science (Washington, DC)* **1989**, *245*, 845. (c) Hickman, J. J.; Ofer, D.; Zou, C.; Laibinis, P. E.; Whitesides, G. M.; Wrighton, M. S. *J. Am. Chem. Soc.* **1991**, *113*, 1128.

(30) Braun, C. M.; Fujishima, A.; Honda, K. *Chem. Lett.* **1985**, 1763.

Proton Affinity Ladders from Variable-Temperature Equilibrium Measurements. 1. A Reevaluation of the Upper Proton Affinity Range

Michael Meot-Ner (Mautner)* and L. Wayne Sieck*

Contribution from the Chemical Kinetics Division, National Institute of Standards and Technology, Gaithersburg, Maryland 20899. *Received October 10, 1990. Revised Manuscript Received January 23, 1991*

Abstract: An interlocking ladder of relative proton affinities of 47 compounds, over a range of 54 kcal/mol, was obtained from the enthalpies of proton-transfer equilibria, by using variable-temperature pulsed high-pressure mass spectrometry. From C_3H_6 (PA = 179.5 kcal/mol) to i-C_4H_8 (PA = 195.9 kcal/mol) the results agree well with tabulated values, but for the upper PA range the present values are increased significantly. For example, the present vs literature PA values are NH_3, 208.3 vs 204.0; CH_3NH_2, 219.6 vs 214.1; and t-$C_4H_9NH_2$, 229.2 vs 220.8 kcal/mol. The new value for t-$C_4H_9NH_2$ is also confirmed by the association thermochemistry of t-$C_4H_9^+$ with NH_3. The entropies of protonation are in reasonable agreement with expected rotational symmetry changes. Aromatics and olefins show a positive entropy of protonation of 3–6 cal/mol K due to structural effects, but no anomalous effects are observed that would indicate a dynamic proton.

Introduction

The gas-phase basicities, i.e., $-\Delta G°$ of protonation, of approximately 800 compounds have been measured, compiled, and evaluated.[1] Most of the data were derived from relative gas-phase basicities (i.e., $\Delta G°$ measurements), as given by the equilibrium constant of reaction 1.

$$AH^+ + B \rightleftarrows BH^+ + A \quad (1)$$

In the great majority of measurements, equilibria 1 were determined at a single temperature, and the thermochemistry was derived from relations 2 and 3.

$$\Delta G° = -RT \ln K \quad (2)$$

$$\Delta G° = \Delta H° - T\Delta S° \quad (3)$$

In order to derive the thermochemistry from measured ln K values, the temperature at which the measurements were done must be assigned. Many of the early ICR measurements were carried out at ambient temperatures, originally assumed to be 300 K. Later, several authors revised their data to take the heating

(1) Lias, S. G.; Liebman, J. F.; Levin, R. D. *J. Phys. Chem. Ref. Data* **1984**, *13*, 695.

of the ICR cell into account. For example, the extensive scale of gas-phase basicity values reported by Taft was expanded by 6% under the assumption that the temperature was actually 320 K. In evaluating these data Lias et al. accepted the revised temperature data recommended by the authors but stated that "In the region above ammonia, the absence of reliable absolute standards makes it impossible to check on the reliability of assigned proton affinity values. If the temperatures at which the measurements were made were not well-known, the thermochemical ladders generated from equilibrium constant determinations could be too long or too short, causing proton affinity values at the top end of the scale to vary considerably from their correct absolute value."[1] In fact, since the proton affinity of ammonia was also considered uncertain, the above statement applies to the scale starting from the comparison standard *i*-C_4H_8 at 195.9 kcal/mol.

With respect to entropy changes, the assumption is usually made[1-3] that most terms which contribute to $\Delta S°_1$ are negligible for most reactant pairs because changes in the moments of inertia and vibrational modes approximately cancel on the two sides of eq 1. In such cases, $\Delta S°_1$ is given by the rotational symmetry change, i.e.,

$$\Delta S°_1 = R \ln [(\sigma_{AH}\sigma_B)/(\sigma_{BH}\sigma_A)] \quad (4)$$

Usually the expected values of $\Delta S°_1$ are 0 to ±2 cal/mol K.

To check assumption 4, variable-temperature equilibrium studies can be used to determine $\Delta H°_1$ and $\Delta S°_1$ directly. Yamdagni and Kebarle tested the validity of eq 4 for several equilibria by using pulsed high-pressure mass spectrometry.[2,3] The accuracy of the entropy measurements was ±2 cal/mol K. The measured entropy changes were mostly in the range 0 to ±2 cal/mol K and agreed with the expected values within the experimental limits.

Larger entropy changes may be expected when the number of rotational degrees of freedom changes, such as in the protonation of monoatomic or linear species.[4] Significant entropy changes may also occur when protonation causes substantial structural changes. This occurs, for example, upon cyclization due to the formation of internal hydrogen bonds and may lead to entropy changes up to 15 cal/mol K.[2,5] Significant entropy changes may also be expected when an olefinic bond is protonated, but measurements by Ausloos and Lias[6] and the present work did not verify this, as will be discussed below.

Except for such special cases, eq 4 can be expected to be a good approximation, and its validity is implicit in the large body of present proton affinity data.[1] However, there are indications that in at least some special cases this assumption may be inaccurate. For example, the protonation of some halotoluenes involved unexpectedly large entropy changes, which were attributed to a mobile proton when halogen substitution decreases the barriers to proton migration around the ring.[7]

A mobile proton in protonated aromatics might contribute substantial positive entropy terms, especially in larger polycyclic ions where the proton could occupy a large free volume. In this case, proton affinities derived by using eq 4 from single temperature studies[8] may be inaccurate. Checking on this situation was one of the motivations for the present work.

In summary, substantial portions of the proton affinity ladder, especially in the upper range, entail uncertainties due to assumptions about temperature and entropy. The present work will reexamine the upper range of proton affinities by using high-pressure conditions with well-defined temperatures and with direct measurements of reaction enthalpies and entropies.

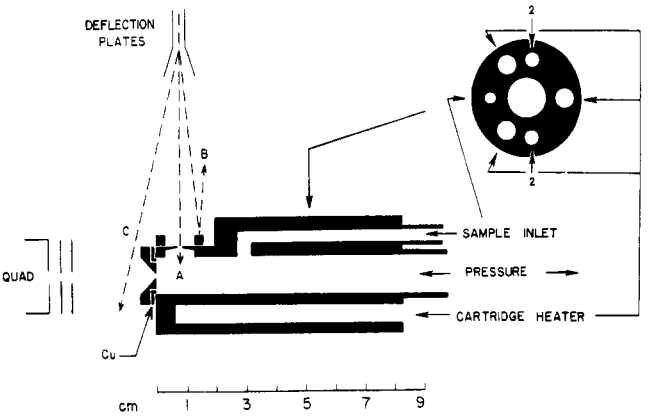

Figure 1. Schematics of the NIST pulsed high-pressure mass spectrometer ion source showing a cross section along the long axis (main diagram) and across, perpendicular to the long axis at midpoint (insert). Position A shows the impact point of the electron beam from an electron gun to penetrate the source for ionization, and B is the position during the nonionizing period of the pulse cycle. Position C is used for quadrupole calibration (see text). The bored-out sections labeled 2 are the cooling channels.

Experimental Section

The measurements were performed by using the NIST pulsed high-pressure mass spectrometer.[9,10] The reaction mixtures were 0.001–0.1% of the compounds of interest in CH_4 as the carrier gas. Trace $CHCl_3$ was added for electron capture to slow ion diffusion. The mixtures were ionized by a 1-ms pulse of 500–1000 eV electrons, and ions diffusing from the source were observed for reaction times of 1–3 ms.

The slopes of the van't Hoff plots, and the derived enthalpies, can be affected by the temperature measurement. As to uniformity of temperature, the body of our current reaction chamber is fabricated from a stainless steel rod approximately 3.8 cm in diameter and 8.4 cm in length (see Figure 1). Uniform heating is provided by three symmetrically placed 60-W cartridge heaters implanted in the cell walls, and cooling of the chamber is accomplished by flowing air or evaporated liquid nitrogen through a bored-out section of the cell body. The reaction volume is defined by a 13-mm diameter hole drilled along the center axis from front to back. No repellers are used, and no potential gradients exist within the reaction volume. The electron entrance and ion exit pinholes are both approximately 60 microns in diameter.

For calibration purposes, cell temperatures are monitored with thermocouples placed at various locations. The primary position is a copper plate compressed between the ion exit assembly (stainless steel) and the cell body (see Figure 1). This plate forms part of the interior front wall of the reaction chamber adjacent to the ion exit pinhole. The ends of fine copper and constantan wires are embedded into this gasket so that it forms one-half of a thermocouple junction with the constantan leads. Usually, this thermocouple is used for temperature measurement. For calibration, temperature readings at the front plate were checked against other thermocouples, both of the copper-constantan and chromel-alumel type, which are positioned to monitor the actual gas temperature in the center of the reaction volume or at various points on the inside wall of the chamber. Deviations between simultaneous readings referenced to the front plate were never more than 1.5 °C throughout the range 170–680 K.

The intercepts of van't Hoff plots could be affected by the mass-dependent transmission of the quadrupole filter and mass-dependent response of the detector. We compensate for discrimination by comparing ionic fragmentation patterns obtained in our instrument with reference spectra. This is accomplished by directing the electron gun to ionize a low-pressure sample in front and outside of the ion exit pinhole (position c in Figure 1). The pressure in this region is in the order of 10^{-6} Torr, where ion–molecule reactions are negligible, and the temperature is adjusted to be equal to the standard reference measurement, usually 250–280 °C. Comparing our detected relative ion intensities to reference 70 eV EI spectra taken with magnetic sector instruments incorporating Faraday Cup detection yields correction factors for our mass discrimination. These checks are repeated periodically to compensate for instrumental drift.

(2) Yamdagni, R.; Kebarle, P. *J. Am. Chem. Soc.* **1973**, *95*, 3504.
(3) Yamdagni, R.; Kebarle, P. *J. Am. Chem. Soc.* **1976**, *98*, 1320.
(4) Fehsenfeld, C.; Lindinger, W.; Schiff, H. I.; Hemsworth, R. S.; Bohme, D. K. *J. Chem. Phys.* **1976**, *64*, 4887.
(5) Meot-Ner (Mautner), M.; Hunter, E. P.; Hamlet, P.; Field, F. H. *J. Am. Chem. Soc.* **1980**, *102*, 6393.
(6) Ausloos, P.; Lias, S. G. *J. Am. Chem. Soc.* **1978**, *100*, 1953.
(7) Fernandez, M. T.; Jennings, K. R.; Mason, R. S. In *Structure/Reactivity and Thermochemistry of Ions*; Ausloos, P., Lias, S. G., Eds.; Proceedings of the NATO ASI Conference, Les Arcs. Reidl, 1986.
(8) Meot-Ner (Mautner), M. *J. Phys. Chem.* **1980**, *84*, 2716.
(9) Meot-Ner (Mautner), M.; Sieck, L. W. *J. Am. Chem. Soc.* **1983**, *105*, 2956.
(10) Sieck, L. W.; Meot-Ner (Mautner), M. *J. Phys. Chem.* **1984**, *88*, 5324.

The reaction mixtures were prepared in a bulb heated to 180 °C and allowed to flow to the ion source through stainless steel tubing heated to 150–180 °C. Most of the compounds were volatile. With less volatile compounds the mixtures were allowed to flow up to 30 min until constant partial pressures were obtained in the ion source. This was checked by the invariance of the measured equilibrium constant with further flow time. The concentrations were also confirmed by kinetic measurements as described below.

Results and Discussion

1. Analysis of Error. a. Errors in $\Delta H°$. van't Hoff plots for proton-transfer equilibria (1) are shown in Figures 2–11 and 13 and for association reactions in Figure 12. The thermochemical data are summarized in Tables I and II. The resulting interlocking proton affinity ladder is shown in Figure 14.

In most of the present measurements, the most significant limitation on accuracy arose from the relatively small temperature range. In general, the useful temperatures were 520–650 K, although several equilibria could be measured down to 450 K. The upper end of the temperature scale was limited by instrumental factors and in some cases by ion decomposition. The limiting low temperature is determined by the occurrence of clustering, which becomes substantial below 520–550 K for most of the oxygen- and cyanide-containing compounds. Fortunately, compounds in the upper PA range, especially amines, pyridines, and vinyl ethers, cluster more weakly, and for these compounds measurements over wider temperature ranges were possible.

The error can be evaluated in several ways. Probably the most reliable check is through measuring $\Delta H°$ scales for values that are well-established by independent methods. For this purpose we measured ladders of $\Delta H°_{ionization}$ and $\Delta H°_{acid}$, as discussed below.

The standard deviation of the slopes and intercepts of the van't Hoff plots yields the error associated with scatter. The average error from this source is ±0.3 kcal/mol for $\Delta H°$ and ±0.6 cal/mol K for $\Delta S°$.

Another check on random error in $\Delta H°$ is the agreement between replicate measurements. For 22 sets of replicate measurements as shown in Table I, the standard deviation from the average is ±0.3 kcal/mol. For the largest set of replicate measurements, (five measurements on $t\text{-}C_4H_9^+ + NH_3$), the standard deviation is ±0.8 kcal/mol. A further measure of the random error in $\Delta H°$ is obtained from the consistency of cycles through the ladder in Figure 13. If the error in each individual value is $\pm h°$ kcal/mol, then for a cycle of n steps the expected error is $n^{1/2}h°$. From the consistency of several cycles in Figure 13, we obtain an average value for $h°$ of ±0.5 kcal/mol.

Systematic errors in $\Delta H°$ may arise from errors in the measurement of the variation of ion source temperature over the range of the temperature studies. Our calibrations as described above indicate that the measured absolute temperatures are accurate at least within ±2 K throughout the temperature range from 270 to 670 K, since measurements at various parts of the source and the use of various types of thermocouples agreed to within ±2 K. Systematic errors such as a temperature gradient through the source would be in the same direction at all temperatures. Therefore, the error in temperature differential between the upper and lower ends of the temperature range, usually 650 and 520 K, is at most 2 K. For a reaction with a typical $\Delta H°$ of 3 kcal/mol, the error would be 0.04 kcal/mol. Therefore the error due to the temperature measurement is negligible.

Another test of the accuracy of our temperature measurements is obtained by comparing $\Delta H°$ values for strongly temperature-dependent systems with data from other sources. Particularly suitable are association equilibria. Table II compares the results for clustering equilibria measured during the present studies with literature values. For three reactions, our $\Delta H°$ values are higher by 4%, 6%, and 3% than the average literature values; one result is identical with, and another one (for $OH^-\cdot H_2O$) is 3% less than, the value which was very carefully redetermined by Kebarle and co-workers.[11] Two further reactions, where no literature data exist, also give the expected results for $(RCN)_2H^+$ and $(R_2CO)H^+$ type dimers.[12,13] These comparisons suggest that our $\Delta H°$ values may be too high by at most 2% assuming that the values from the other laboratories are accurate. This would introduce an error of only 0.2 kcal/mol to the measured ΔPA of 12.4 kcal/mol from $i\text{-}C_4H_8$ to NH_3 and 0.7 kcal/mol to the ΔPA of 36.8 kcal/mol between $i\text{-}C_4H_8$ and $(CH_3)_3N$.

Another possible source of error would occur if ln K changed during a temperature study due to a variation in mixture composition. The temperature studies were usually conducted by going from high to lower temperatures. To check against composition drift, the temperature was raised after the end of the temperature study to confirm that the ln K measured at the original high-temperature point had not changed significantly.

b. Errors in $\Delta G°$. The value of $\Delta G°$ is determined by using eq 5.

$$\Delta G° = -RT \ln K = -RT \ln \frac{I(BH^+)P(A)}{I(AH^+)P(B)} \qquad (5)$$

Random errors in $\Delta G°$ may arise from the measurement of the relative partial pressures $P(A)$ and $P(B)$. One test of composition is the use of reaction kinetics. With the low concentrations of reactants used in the present studies, the approach to equilibrium was observed in most reactions, and rate constants were measured. The measured rate constants for exergonic reactions as calculated by using the nominal concentrations were usually equal to the expected collision rates. This indicates that the actual reactant concentrations in the ion source were equal within ±30% to the nominal concentrations.

Another measure of errors in reactant concentrations is the reproducibility of ln K in experiments with various mixture compositions. Variation of mixture composition was performed routinely for most equilibria. When $P(A)/P(B)$ was varied up to a factor of 10, the average reproducibility of ln K was ±0.3, corresponding to ±0.4 kcal/mol for $\Delta G°$ at 600 K.

Errors in $\Delta G°$ may also arise from errors in the measured ion signal intensity ratio $I(BH^+)/I(AH^+)$. Random error in this quantity may arise from tuning the mass analyzer off the maxima of peaks and from variation of signal intensities during the measurement. These errors are minimized by a procedure that involves measuring $I(AH^+)$, followed by $I(BH^+)$, retuning, and remeasuring $I(BH^+)$. The random error in $\Delta G°$ can be estimated from the standard deviation in replicate measurements. The average standard deviation for 20 systems is ±0.3 kcal/mol. The standard deviation in the largest set of data, five measurements on $t\text{-}C_4H_9^+ + NH_3$, is ±0.7 kcal/mol.

Systematic errors in $\Delta G°$ may also arise from mass discrimination in the quadrupole mass analyzer and in the detector. Discrimination by the mass analyzer was compensated for by comparing ion intensities at decreasing resolution, until $I(BH^+)/I(AH^+)$ does not vary further with resolution. The overall mass discrimination was calibrated as described in the Experimental Section. The largest discrimination occurred against low mass ions. For example, in the reaction pair $NH_4^+/c\text{-}C_3H_5COCH_3^+$ (m/z 18/84), the required correction is by a factor of 3.6, corresponding to a correction in ln K of 1.3, i.e., a correction of 2.6 cal/mol K in $\Delta S°$ and 1.6 kcal/mol in $\Delta G°_{600}$.

Further calibration of the accuracy of the $\Delta H°$ and $\Delta G°$ scales was done by measuring a scale of ionization energies as discussed below.

c. Errors in $\Delta S°$. The values of $\Delta S°$ are calculated from the relation $\Delta S° = (\Delta H° - \Delta G°)/T$. Combining the estimated error of ±0.5 kcal/mol in $\Delta H°$ and ±0.4 kcal/mol in $\Delta G°$ yields an expected error in $\Delta S°$ of about ±1.2 cal/mol K. In fact, the observed precision is somewhat higher. The average standard deviation in 21 replicate measurements is ±0.6 cal/mol K, and the standard deviation in five measurements of $t\text{-}C_4H_9^+ + NH_3$

(11) Kebarle, P. Private communication, September 1989.

(12) Speller, C. V.; Meot-Ner (Mautner), M. *J. Phys. Chem.* **1985**, *81*, 5217.

(13) Meot-Ner (Mautner), M. *J. Am. Chem. Soc.* **1984**, *106*, 1257.

is ±0.5 cal/mol K. On this basis, we estimate the error in $\Delta S°$ as ±0.6 cal/mol K.

In summary, the estimated errors in the measured thermochemistry of a proton transfer equilibrium are ±0.5 kcal/mol in $\Delta H°$, ±0.4 kcal/mol in $\Delta G°$, and ±0.6 cal/mol K in $\Delta S°$.

d. Estimates of Accuracy from the Comparison of the $\Delta H°$ and $\Delta G°$ Scales and from Calibration by IP and Acidity Scales. As we noted above, the $\Delta H°$ and $\Delta G°$ measurements have different and independent sources of error. For example, an error in measuring temperature differentials will affect $\Delta H°$ only, while errors in absolute temperatures, mixture composition, and mass discrimination will affect $\Delta G°$ only. Comparing the PA and $\Delta G°_{600}$ scales in Figure 14 is therefore a good test of accuracy.

In fact, the two scales agree well. For example, the difference in $\Delta G°_{600}$ between CH_3CN and pyridine, which are both well-anchored into the ladder and exhibit no significant entropy effects, is 38.1 kcal/mol, compared with a $\Delta H°$ difference of 39.0 kcal/mol.

To further test the accuracy of $\Delta H°$ ladders measured with our apparatus, we constructed a ladder of charge-transfer equilibria yielding relative ionization energies for aromatic molecules whose IPs are well-known from spectroscopy. The scale extends from aniline to naphthalene, toluene, benzene, and C_6F_6. Over the scale our measurements give an IP difference of 49.1 kcal/mol, compared with 50.9 kcal/mol from spectroscopic values. The $\Delta H°$ and $\Delta G°$ scales for ionization energies agree closely. These data do not indicate any artifacts that would cause an apparent expansion of our scales. These results will be reported in detail elsewhere.[14]

We also constructed a scale of proton-transfer equilibria in anions. The range extends from H_2S to H_2O and agrees well with the spectroscopic relative $\Delta H°_{acid}$ values for these reference compounds, separated by a range of nearly 48 kcal/mol. Here also the $\Delta G°$ scale agrees well with the $\Delta H°$ scale and with published gas-phase acidity scales, within 1 kcal/mol over a range of 50 kcal/mol.

Our PA, IP, and $\Delta H°_{acid}$ ladders and the corresponding $\Delta G°$ ladders all span a range of about 50 kcal/mol. Comparison with reference standards in the IP and $\Delta H°_{acid}$ scales and the agreement between the $\Delta H°$ vs $\Delta G°$ scales suggest that our equilibrium $\Delta H°$ and $\Delta G°$ ladders measure the energy span over a range of 50 kcal/mol with an accuracy of ±2 kcal/mol.

2. Proton Affinities. An analysis of the network of values in Figure 14 was performed by using the NIST statistical program for overdetermined thermochemical networks. The results yield a PA ladder, i.e., relative values of $-\Delta H°_{protonation}$ at 600 K. These values must be extrapolated to approximately 300 K to compare with the bulk of existing data from ICR measurements and to 0 K where they are anchored to threshold values for reference compounds.

Data for the heat capacities of protonated species are lacking but may be approximated by neutral analogues. For example, ROH_2^+ may be estimated by RNH_2, $(CH_3)_2NH_2^+$ by $(CH_3)_2CH_2$, etc. Using such models and thermochemical tables[15] shows that $\Delta H°(600) - \Delta H°(300)$ for exothermic reactions (eq 1) is less than 0.5 kcal/mol. (These corrections are not cumulative, i.e., the same applies for any reactant pair regardless of how far removed on the PA ladder.) The corrections decrease with temperature, and therefore even the $\Delta H°(600) - \Delta H°(0)$ difference is probably less than 0.5 kcal/mol. We therefore assume that for most reactions involving no significant structural changes, the measured values of $\Delta H°$ apply down to 0 K, and the PA scale is not significantly affected by temperature. In fact, no curvature in the van't Hoff plots was noted in any temperature studies of proton transfer, even when the temperature was varied over a wide range, for example, from 360 to 650 K in the azuleneH$^+$ + *N,N*-dimethylaniline system, Figure 6a.

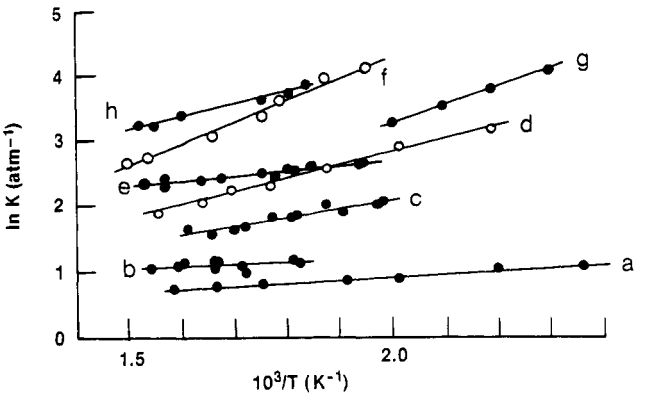

Figure 2. van't Hoff plots for proton-transfer equilibria between the reactants: a. $C_6H_5NH_2H^+$ + 2-Fpyridine; b. $CH_3OH_2^+ + C_6H_6$; c. i-$C_3H_7^+ + CH_3OH$; d. $C_6H_7^+ + CH_3CHO$; e. $CH_3CNH^+ + C_6H_5CH_3$; f. $C_6H_7^+ + CH_3CN$; g. $C_6H_7^+ + CH_3SH$; h. $CH_3CNH^+ + C_2H_5CN$.

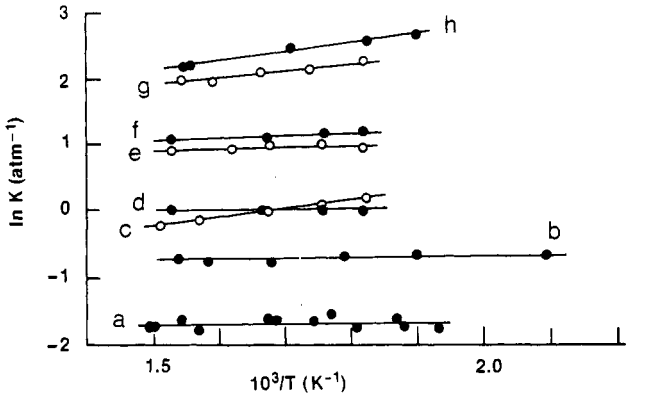

Figure 3. van't Hoff plots for proton-transfer equilibria between the reactants: a. $C_6H_5CH_3H^+ + CH_2CHCN$; b. pyridineH$^+$ + $(CH_3)_2NH$; c. $C_6H_5CH_3H^+ + C_2H_5CN$; d. $HCOOCH_3H^+ + CH_2CHCN$; e. $CH_3CNH^+ + CH_2CHCN$; f. $CH_3CNH^+ + HCOOCH_3$; g. pyrroleH$^+$ + 2-Fpyridine; and h. $CH_3COOCH_3H^+ + CH_3SCH_3$.

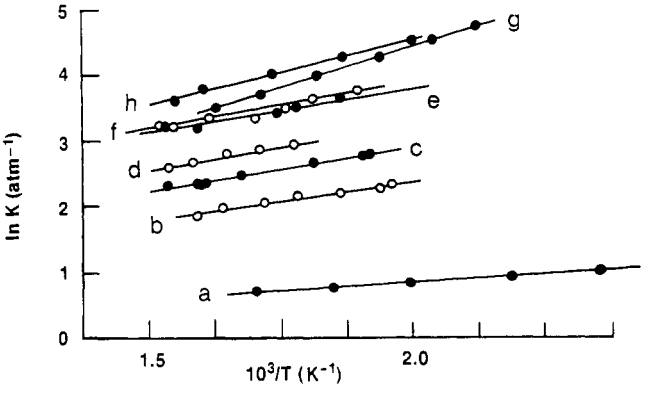

Figure 4. van't Hoff plots for proton-transfer equilibria between the reactants: a. $CH_3NH_3^+$ + thiazole; b. $HCOOCH_3H^+ + C_2H_5CN$; c. i-$C_3H_7CNH^+ + (CH_3)_2CO$; d. $C_2H_5CNH^+ + i$-C_3H_7CN; e. $CH_2CHCNH^+ + CH_3OCH_3$; f. $(CH_3)_2COH^+$ + 1-methylnaphthalene; g. thiazoleH$^+$ + i-$C_3H_7NH_2$; and h. pyridineH$^+$ + $(CH_3)_3N$.

An exception to the negligible Δc_p values may be in the half-reaction t-$C_4H_9^+ \rightarrow i$-C_4H_8. Here the elimination of an internal rotor may increase significantly the energy of the ion vs the neutral in going from 300 to 600 K. This would decrease the proton affinity. For the half-reaction $(CH_3)_3C^+ \rightarrow (CH_3)_2C{=}CH_2$, the ion can be modeled by $(CH_3)_3CH$ or $(CH_3)_3N$. Thermochemical tables[15] then show that $\Delta H°_{600} - \Delta H°_{300} = -1.1$ or -0.5 kcal/mol, respectively. On the other hand, protonation of lone-pair donors $B \rightarrow BH^+$, with c_p values estimated by neutrals as above, makes a positive contribution of 0.1–0.5 kcal/mol to $\Delta H°_{600} - \Delta H°_{300}$. These estimates suggest that the PA of i-C_4H_8 should decrease

(14) Meot-Ner (Mautner), M.; Sieck, L. W. *Int. J. Mass Spectrom. Ion Processes* Submitted for publication.

(15) Stull, D. R.; Westrum, E. F.; Sinke, G. C. *The Chemical Thermodynamics of Organic Compounds*; Wiley: New York, 1969.

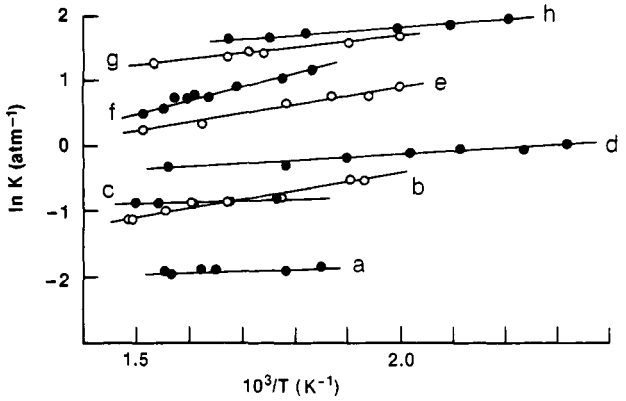

Figure 5. van't Hoff plots for proton-transfer equilibria between the reactants: a. naphthaleneH$^+$ + i-C_3H_7CN; b. naphthaleneH$^+$ + i-C_4H_8; c. t-$C_4H_9^+$ + i-C_3H_7CN; d. azuleneH$^+$ + pyridine; e. 1-methylnaphthaleneH$^+$ + $(C_2H_5)_2CO$; f. naphthaleneH$^+$ + $(CH_3)_2CO$; and g. t-$C_4H_9^+$ + $(CH_3)_2CO$.

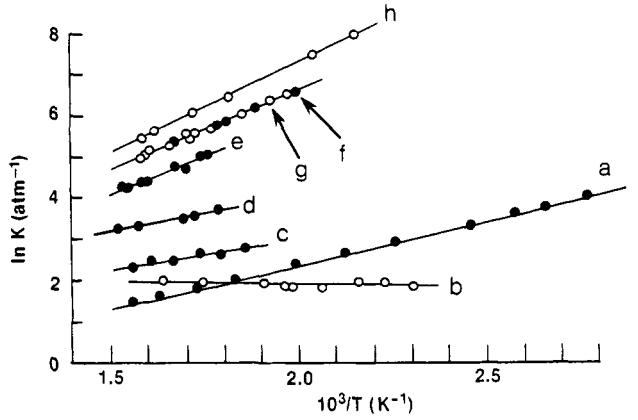

Figure 6. van't Hoff plots for proton-transfer equilibria between the reactants: a. azuleneH$^+$ + N,N-dimethylaniline; b. i-$C_3H_7NH_3^+$ + azulene; c. $CH_3OCH_3H^+$ + i-C_4H_8; d. CH_2CHCNH^+ + CH_3OCH_3; e. t-$C_4H_9^+$ + CH_3SCH_3; f. t-$C_4H_9^+$ + $CH_3COOC_2H_5$; and g. t-$C_4H_9^+$ + $(C_2H_5)_2CO$.

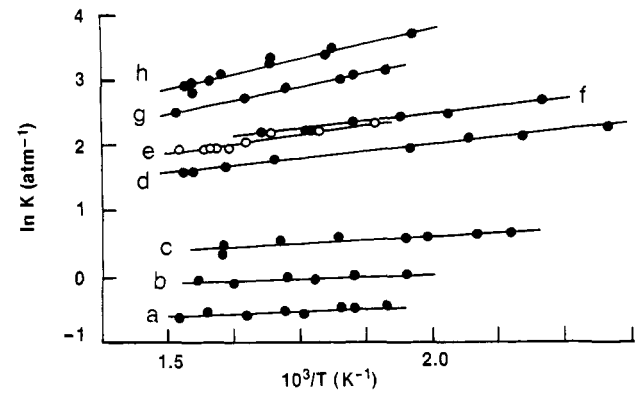

Figure 7. van't Hoff plots for proton-transfer equilibria between the reactants: a. t-$C_4H_9^+$ + i-C_3H_7CN; b. $(CH_3)OH^+$ + C_2H_5CN (intercept arbitrary); c. $CF_3CH_2NH_3^+$ + NH_3; d. oxazoleH$^+$ + 2-Fpyridine; e. CH_3CHOH^+ + CH_3CN; f. $CF_3CH_2NH_3^+$ + c-$C_3H_5COCH_3$; g. $(CH_3)_2OH^+$ + i-C_3H_7CN (intercept arbitrary); and h. c-$C_3H_5COCH_3^+$ + pyrrole.

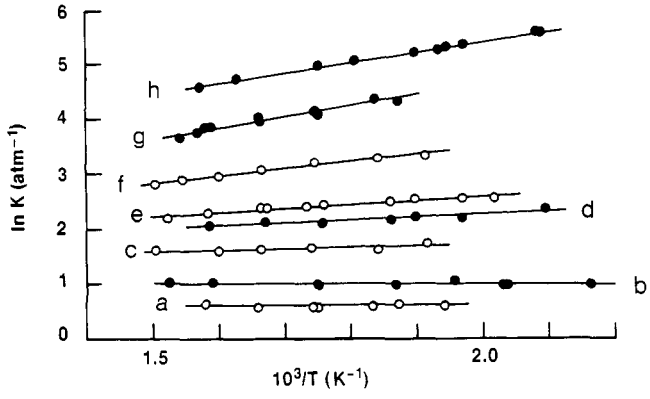

Figure 8. van't Hoff plots for proton-transfer equilibria between the reactants: a. pyrroleH$^+$ + oxazole; b. $C_6H_5NH_2H^+$ + 2-Fpyridine; c. $(CH_3)_2COH^+$ + CH_3COOCH_3; d. NH_4^+ + c-$C_3H_5COCH_3$; e. $CF_3CH_2NH_3^+$ + c-$C_3H_5COCH_3$; f. t-$C_4H_9^+$ + CH_3COOCH_3; g. c-$C_3H_5COCH_3H^+$ + oxazole; and h. $C_2H_5NH_3^+$ + pyridine.

vs other bases by 0.4–1.6 kcal/mol in going from 300 to 600 K. Similar effects are expected also in the protonation of C_3H_6, styrene, and the vinyl ethers.

Nevertheless, the present measured 600 K PA of i-C_4H_8 vs nearby compounds such as CH_3OCH_3 and i-C_3H_7CN does not differ significantly from the tabulated relative PA values which were measured mostly at 300–400 K. Therefore, since the c_p effect is not known accurately, we shall use the recommended value[1] for 300 K, PA(i-C_4H_8) = 195.9 ± 1.5 kcal/mol as the reference value at 600 K, and also use PA(C_3H_6) = 179.5 ± 0.8 kcal/mol.[1] At most, the absolute PA values based on i-C_4H_8 in Figure 13 at 600 K need to be decreased by about 1 kcal/mol to calculate absolute PAs at 300 K and by about 1.5 kcal/mol to calculate absolute 0 K PA values.

The absolute PA of C_3H_6 is known more accurately than of i-C_4H_8. However, i-$C_3H_7^+$ reacts with C_3H_6, and because of this complicating reaction we succeeded to measure C_3H_6 only vs one other compound, CH_3OH. Even this one link to the ladder was further complicated by the strong clustering of $CH_3OH_2^+$, which limited the temperature range for equilibrium studies. This resulted in an inconsistency of 1.3 kcal/mol in the CH_3OH–C_6H_6–C_6H_5F cycle. Fortunately, however, the i-$C_3H_7^+$ ion was also interrelated to the proton affinity scale through condensation reactions as described below. Nevertheless, we use i-C_4H_8 as the reference for the whole network.

3. Vinyl Ethers as Absolute Proton Affinity Standards. As noted above, the main problem is the lack of absolute standards in the upper PA range. Such standards could be provided by vinyl ethers. The protonated species, which are oxocarbonium ions, can be also obtained as fragments from saturated ethers, and the heats of formation can be derived from appearance potentials.

The ion $CH_3CHOCH_3^+$ can be obtained from the protonation CH_2CHOCH_3 or by ionization and the loss of R = H or CH_3 from $CH_3CH(R)OCH_3$, with appearance potential AP. The proton affinity is then calculated from eq 6.

$$PA(CH_2CHOCH_3) = -AP + \Delta H°_f(CH_2CHOCH_3) - \Delta H°_f(CH_3CH(R)OCH_3) + \Delta H°_f(R) + \Delta H°_f(H^+) \quad (6)$$

$\Delta H°_f(CH_2CHOCH_3)$ was estimated as −24 kcal/mol, probably with an accuracy of ±2 kcal/mol.[1] For R = H, Lossing measured the AP as 238 ± 2 kcal/mol,[16] and $\Delta H°_f(CH_3CH_2OCH_3)$ = −51.7 kcal/mol.[1] For R = CH_3, Lossing measured the AP as 227 ± 2 kcal/mol,[16] and $\Delta H°_f((CH_3)_2CHOCH_3)$ = −60.2 kcal/mol.[1] With these data, eq 6 gives PA(CH_2CHOCH_3) = 207.5 and 209.7 kcal/mol. The average valve of 208–209 kcal/mol is in good agreement with the position of CH_2CHOCH_3 in the ladder at 208.5 kcal/mol.

A similar approach can be used for $CH_2C(CH_3)OCH_3$. The value of AP$(CH_3)_2COCH_3^+$ from $(CH_3)_3COCH_3$ was measured by Lossing as 218.2 kcal/mol.[16] An uncertainty exists in $\Delta H°_f(CH_2C(CH_3)OCH_3)$, which is estimated as −34.2 kcal/mol from Benson's tables[17] and as −36 kcal/mol from group substitution methods. By using $\Delta H°_f((CH_3)_3COCH_3)$ = −67.8 kcal/mol,[1] an equation analogous to eq 6 gives PA($CH_2C(CH_3)OCH_3$) = 215 ± 4 kcal/mol. This is lower by 3 kcal/mol than the position in the present ladder.

In summary, vinyl ethers are good candidates for absolute standards in upper PA range, but better thermochemical data are

(16) Lossing, F. P. *J. Am. Chem. Soc.* **1979**, *99*, 7526.

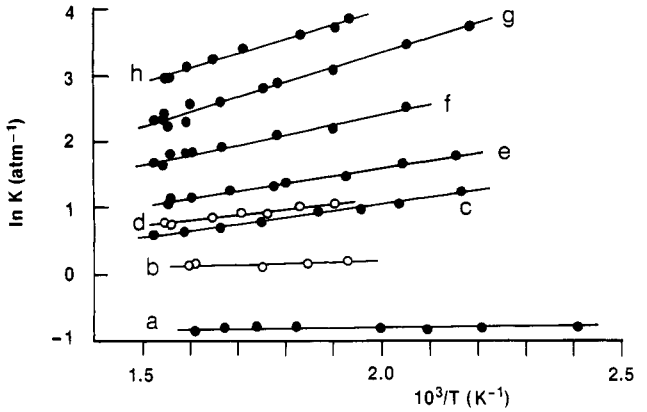

Figure 9. van't Hoff plots for proton-transfer reactions between the reactants: a. pyridineH^+ + $(CH_3)_2NH$; b. thiazoleH^+ + 3-Fpyridine; c. oxazoleH^+ + $C_6H_5NH_2$; d. $(CH_3)_2SH^+$ + $(C_2H_5)_2CO$; e. 3-FpyridineH^+ + $C_2H_5NH_2$; f. 2-FpyridineH^+ + CH_3NH_2; g. 2-FpyridineH^+ + thiazole; and h. $CH_3COOCH_3H^+$ + $(C_2H_5)CO$.

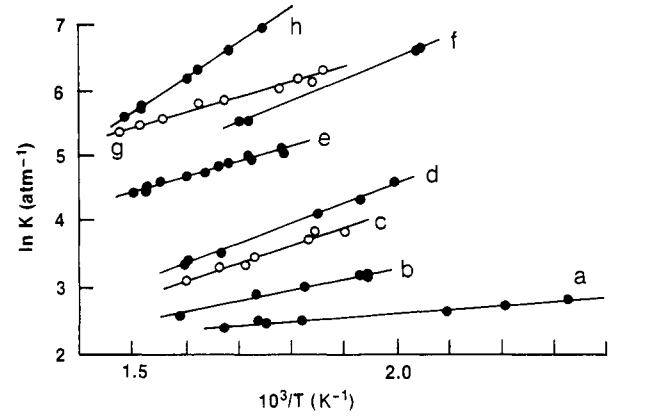

Figure 10. van't Hoff plots for proton-transfer equilibria between the reactants as follows: a. i-$C_3H_7NH_3^+$ + pyridine; b. $C_2H_5NH_3^+$ + i-$C_3H_7NH_2$; c. $(CH_3)_2SH^+$ + NH_3; d. 3-FpyridineH^+ + i-$C_3H_7NH_2$; e. c-$C_3H_5COCH_3H^+$ + $C_6H_5NH_2$; f. $C_2H_5NH_3^+$ + t-$C_4H_9NH_2$; g. NH_4^+ + pyrrole; and h. t-$C_4H_9NH_3^+$ + $CF_3CH_2NH_2$.

required for the needed accuracy of at least ±2 kcal/mol.

4. Free Energies and Entropies. The $\Delta G°_{600}$ values are in good agreement with the $\Delta H°$ scale. For example, the $\Delta H°$ difference between acetonitrile and trimethylamine is 44.1 kcal/mol, while the $\Delta G°$ difference is 42.8 kcal/mol. As discussed above, the two scales are independent in terms of the sources of error. Given the fact that the compounds at the upper range are connected to the reference compound i-C_4H_8 through 8–10 steps, the difference of 1.3 kcal/mol is small, considering the cumulative error.

The experimental $\Delta S°$ values are compared with $\Delta S°_{rot.\,sym}$ in Table I. Most rotational symmetry numbers for the ions can be assigned without ambiguity, except for a few cases noted in Table I. In assigning symmetry numbers, the symmetries of internal rotors are significant. For example, a $-CH_3$ or $-NH_3$ group formed by the protonation of olefins and amines makes an entropy contribution of $-R$ ln 3 = −2.2 cal/mol K, which may be a significant part of the total entropy change.[17]

The last column in Table I shows the differences between the experimental $\Delta S°$ and $\Delta S°_{rot.\,sym}$ (a positive value shows that the experimental value is more positive than expected). These entropy factors are denoted as $\Delta S°_{structural}$. This term includes the entropy changes due to structural effects, other than symmetry, and also experimental error. This term is experimentally meaningful if greater than ±2 cal/mol K.

For olefins, we find that the overall entropy of protonation is only slightly positive, in agreement with the results of Ausloos and Lias.[6] These values are somewhat unexpected, since the process creates a new free rotor. The result can be explained by the internal symmetry of the new CH_3 rotors. When this entropy effect, i.e., $\Delta S°_{rot.\,sym} = -R$ ln 3 is accounted for, then the $\Delta S°_{structural}$ term in Table I is about 3 cal/mol K in the protonation of C_3H_6, 4.5 cal/mol K in styrene, and 4–6 cal/mol K cal/mol K in the protonation of i-C_4H_8 and the vinyl ethers. These entropy changes are consistent with the rotational entropy of the new $-CH_3$ rotor which is expected to be 4–6 cal/mol K.[17]

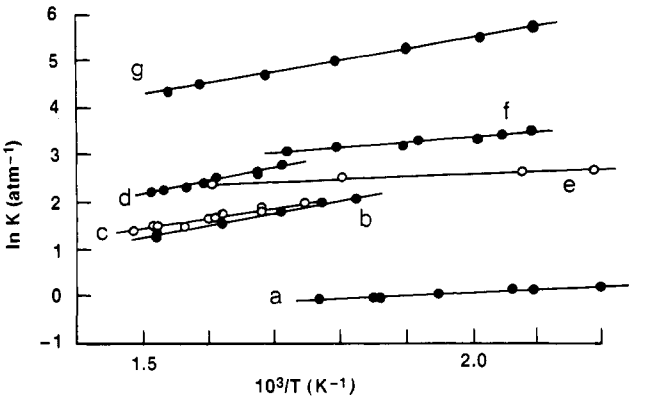

Figure 11. van't Hoff plots for proton-transfer equilibria between the reactants: a. pyridineH^+ + t-$C_4H_9NH_2$; b. $(C_2H_5)_2COH^+$ + NH_3; c. $(CH_3)_2SH^+$ + $CF_3CH_2NH_2$; d. $CH_3COOC_2H_5H^+$ + NH_3; e. $CH_3NH_3^+$ + 3-Fpyridine; f. i-$C_3H_7NH_3^+$ + t-$C_4H_9NH_2$; and g. $(CH_3)_2NH_2^+$ + $(CH_3)_3N$.

For $C_6H_6 \rightarrow C_6H_7^+$, $\Delta S°_{rot.\,sym} = R$ ln (12/2) = 3.6 cal/mol K. $\Delta S°$ was determined against CH_3OH, CH_3CHO, CH_3SH, and CH_3CN, and for all of these compounds $\Delta S°_{rot.\,sym}$ (A → AH^+) = 0. The average $\Delta S°$ for these reactions is 3.1 ± 1.5 cal/mol K, in good agreement with the expected value. The result is also in agreement with the results of Lau, who measured the proton-transfer equilibrium between C_6H_6 and C_2H_5OH,[18] and of Lau and Kebarle[19] and Bohme et al.[20] for proton transfer between C_6H_6 and C_6H_5F. For the protonation of toluene, naphthalene, and azulene, the value of $\Delta S°_{structural}$ in several reactions is about 2–3 cal/mol K.

For $NH_3 \rightarrow NH_4^+$, $\Delta S°_{rot.\,sym} = R$ ln (3/12) = −2.8 cal/mol K. Full statistical mechanical calculations or estimation of $\Delta S°(NH_4^+)$ by that of $\Delta S°(CH_4)$ gives similar values,[15] −1.5 cal/mol K at 300 K and −1 cal/mol K at 600 K. Measured against $(CH_3)_2S$, $CH_3COOC_2H_5$, $(C_2H_5)_2CO$, $C_6H_5COCH_3$, and pyrrole, after accounting for $\Delta S°_{rot.\,sym}$ of the reference compounds, our results give $\Delta S°$ ($NH_3 \rightarrow NH_4^+$) = −2.4 ± 1.2 cal/mol K in agreement with the expected value. However, $\Delta S°$ for t-$C_4H_9^+$ + $NH_3 \rightarrow NH_4^+$ + i-C_4H_8 is −6.2 cal/mol K (Table I), somewhat more negative than expected from the other results. McMahon recently found a similar result for this reaction.[21] We note that $\Delta S°$ for reactions involving ammonia are difficult to measure accurately because of gas adsorption problems and large mass differences between the reactant and product ions.

The experimental $\Delta S°$ for $RNH_2 \rightarrow RNH_3^+$ half-reactions is generally −2 to −3 cal/mol K, in agreement with the change of the internal rotational symmetry of the amine group. ($\Delta S°_{rot.\,sym} = R$ ln 1/3 = −2.2 cal/mol K.)

In general, the results in Table I show that the measured $\Delta S°_{experimental}$ values for proton-transfer equilibria, as obtained from the intercepts of the van't Hoff plots or equivalently from $(\Delta H°_{experimental} - \Delta G°_{600})/T$, are small and in good agreement with symmetry and structural considerations.

The values of $\Delta S°_{structural}$ in Table I were derived from individual equilibria. Another alternative would be to calculate the entropies

(17) Benson, S. W. *Thermochemical Kinetics*; John Wiley and Sons: New York, 1976.

(18) Lau, Y. K. Ph.D. Thesis, University of Alberta, Calgary, Alberta, Canada, 1979. Kebarle, P.; Lau, Y. K. *J. Am. Chem. Soc.* **1976**, *98*, 7452.

(19) Davidson, W. R.; Lau, Y. K.; Kebarle, P. *Can. J. Chem.* **1978**, *56*, 1016.

(20) Bohme, D. K.; Stone, J. A.; Mason, R. S.; Stradling, R. S.; Jennings, K. R. *Int. J. Mass Spectrom. Ion Phys.* **1981**, *37*, 283.

(21) McMahon, T. B. Private communication, 1990.

Table I. Thermochemistry of Proton-Transfer Equilibria[a]

reaction	$\Delta H°$	$\Delta S°$	$\Delta G°_{600}$[b]	$\Delta S°_{\text{rot. sym}}$[c]	$\Delta S°_{\text{structural}}$[c,d]
i-$C_3H_7^+$ + CH_3OH	−2.7	−1.2	−2.0	+2.2[e,f]	−3.4
$CH_3OH_2^+$ + C_6H_6	−0.1	+2.2	−1.4		
	−0.6	+1.1	−1.3		
	(−0.3)	(+1.6)	(−1.3)	+3.6	−2.0
$CH_3OH_2^+$ + C_6H_5F	−0.2	+0.8	−0.7	0[g]	+0.8
$C_6H_7^+$ + C_6H_5F	−1.2	−3.7	+1.0	−3.6[g]	−0.1
$C_6H_7^+$ + CH_3CHO	−4.0	−2.3	−2.6	−3.6	+1.3
$C_6H_7^+$ + CH_3SH	−5.3	−4.0	−2.9[h]		
$C_6H_7^+$ + CH_3CN	−6.6	−4.6	−3.8	−3.6	−1.0
$C_6H_7^+$ + $C_6H_5CH_3$	−8.3	−2.0	−7.1	−2.2	+0.2
CH_3CHOH^+ + CH_3CN	−2.9	−0.6	−2.5	0	−0.6
CH_3CNH^+ + $C_6H_5CH_3$	−1.2	+2.8	−2.9		
	−1.9	+1.6	−2.9		
	(−1.6)	(+2.2)	(−2.9)	+1.4	+0.9
CH_3CNH^+ + C_2H_5CN	−3.8	+0.6	−4.2	0	+0.6
CH_3CNH^+ + CH_2CHCN	−0.6	+0.8	−1.1	0	+0.8
CH_3CNH^+ + $HCOOCH_3$	−0.6	+1.3	−1.4	0	+1.3
$HCOOCH_3H^+$ + CH_2CHCN	−0.1	+0.1	−0.2	0	+0.1
$HCOOCH_3H^+$ + C_2H_5CN	−3.1	−1.0	−2.5	0	−1.0
$C_6H_5CH_3H^+$ + CH_2CHCN	−0.1	−3.5	+2.0	−1.4	−2.1
$C_6H_5CH_3H^+$ + C_2H_5CN	−2.7	−4.5	0.0		
	−2.9	−2.2	−1.6		
	(−2.8)	(−3.4)	(−0.8)	−1.4	−2.0
$C_6H_5CH_3H^+$ + i-C_3H_7CN	−5.1	−1.7	−4.1		
CH_2CHCNH^+ + $(CH_3)_2O$	−3.4	+1.2	−4.1	+1.4	−0.2
$(CH_3)_2OH^+$ + C_2H_5CN	−0.7	NA[h]	NA[h]		
$(CH_3)_2OH^+$ + i-C_4H_8	−3.2	−0.4	−3.0	−5.8	+5.4
	−3.7	NA[h]	NA[h]		
	(−3.5)				
$C_2H_5CNH^+$ + i-C_3H_7CN	−2.4	+0.2	−2.3	0	+0.2
naphthaleneH$^+$ + i-C_3H_7CN	−0.5	−4.6	+2.3	−2.8	−2.0
naphthaleneH$^+$ + $(CH_3)_2CO$	−4.0	−5.0	−1.0	−1.4	−3.6
i-$C_3H_7CNH^+$ + i-C_4H_8	−0.9	+0.5	−1.2	−4.4	+4.9
i-$C_3H_7CNH^+$ + $(CH_3)_2CO$	−3.7	−1.1	−3.0		
	−3.3	−0.6	−2.9		
	(−3.5)	(−0.9)	(−2.9)	−1.4	−0.3
t-$C_4H_9^+$ + $(CH_3)_2CO$	−1.9	−0.3	−1.7		
	−2.2	−0.8	−1.7		
	−2.4	−1.1	−1.7		
	(−2.2)	(−0.7)	(−1.7)	+5.8[e,f]	−6.5
t-$C_4H_9^+$ + CH_3COOCH_3	−3.1	+0.9	−3.6	+4.4[e,f]	−3.5
t-$C_4H_9^+$ + $(CH_3)_2S$	−6.4	−1.2	−5.7		
	−7.3	−2.9	−5.6		
	(−6.8)	(−2.1)	(−5.7)	+5.8[e,f]	−7.9
t-$C_4H_9^+$ + $CH_3COOC_2H_5$	−7.7	−2.2	−6.5	+4.4[e,f]	−6.6
t-$C_4H_9^+$ + $(C_2H_5)_2CO$	−7.4	−1.8	−6.3	+5.8[e,f]	−7.6
t-$C_4H_9^+$ + $CF_3CH_2NH_2$	−9.6	−3.6	−7.4		
	−10.8	−5.0	−7.8		
	(−10.2)	(−4.3)	(−7.6)	+2.2[e,f]	−6.5
t-$C_4H_9^+$ + NH_3	−13.0	−6.9	−8.9		
	−13.6	−6.5	−9.7		
	−13.0	−5.8	−9.5		
	−12.2	−5.8	−8.7		
	−12.1	NA[i]	NA[i]		
	(−12.8)	(−6.2)	(−9.0)	+1.6[e,f]	+7.7
$(CH_3)_2SH^+$ + $CF_3CH_2NH_2$	−4.3	−3.5	−2.2	−3.6	+0.1
$(CH_3)_2COH^+$ + CH_3COOCH_3	−0.7	+2.0	−1.9	−1.4	+3.4
$(CH_3)_2COH^+$ + 1-methylnaphthalene	−3.6	NA[i]	NA[i]	−1.4	+2.4
$(CH_3)_2COH^+$ + $C_6H_5CHCH_2$	−5.7	+1.0	−6.3	−3.6	+4.6
$CH_3COOCH_3H^+$ + $(CH_3)S$	−2.9	−0.1	−2.8	+1.4	−1.5
$CH_3COOCH_3H^+$ + $(C_2H_5)_2CO$	−4.5	−1.0	−3.9	+1.4	−2.5
1-methylnaphthaleneH$^+$ + $(C_2H_5)_2CO$	−2.8	NA	NA	+1.4	−5.4
$(CH_3)_2SH^+$ + $(C_2H_5)_2CO$	−1.8	−1.2	−1.1	0	−1.2
$(CH_3)_2SH^+$ + NH_3	−5.5	−2.6	−3.9	−4.2	+1.6
$CH_3COOC_2H_5H^+$ + NH_3	−5.5	−3.8	−3.2	−2.8	−1.0
$(C_2H_5)_2COH^+$ + $C_6H_5CHCH_2$	−0.4	+0.8	−0.9	−3.6	+4.4
$C_2H_5COC_2H_5H^+$ + indene	−2.7	+1.2	−3.4	−1.4	+2.6
$(C_2H_5)_2COH^+$ + NH_3	−5.2	−5.2	−2.1	−4.2	−1.0
$C_6H_5CHCH_3^+$ + indene	−3.6	−1.2	−2.9[h]	+2.2[f]	−3.4
$C_6H_5CHCH_3^+$ + $C_6H_5COCH_3$	−5.5	−1.0	−4.9	+2.2[f]	−3.2
indeneH$^+$ + $C_6H_5COCH_3$	−3.0	−1.7	−2.0[h]		
	−2.2	−0.2	−2.1		
	(−2.6)	(−1.0)	(−2.0)	0	−1.0
$CF_3CH_2NH_3^+$ + NH_3	−1.0	NA[i]	NA[i]		
$CF_3CH_2NH_3^+$ + c-$C_3H_5COCH_3$	−1.5	+2.1	−2.7		
	−2.3	+0.6	−2.8		
	(−1.9)	(+1.4)	(−2.8)	+2.2[f]	−0.8

Table I (Continued)

reaction	$\Delta H°$	$\Delta S°$	$\Delta G°_{600}$[b]	$\Delta S°_{rot.\,sym}$[c]	$\Delta S°_{structural}$[c,d]
$CF_3CH_2NH_3^+ + CH_2CHOCH_3$	−2.8	+4.9	−5.7		
	−3.4	+3.4	−5.4		
	−2.8	+5.1	−5.9		
	−3.4	+4.0	−5.8		
	(−3.1)	(+4.4)	(−5.7)	0[e,f]	+4.4
$NH_4^+ + CH_2CHOCH_3$	−0.2	NA[l]	NA[l]		
$NH_4^+ + C_6H_5COCH_3$	−2.1	+1.1	−2.9	+2.8	−1.7
$NH_4^+ + c\text{-}C_3H_5COCH_3$	−0.9	NA[l]	NA[l]		
$NH_4^+ +$ pyrrole	−5.2	+2.4	−6.6		
	−4.8	+3.6	−7.0		
	(−5.0)	(+3.0)	(−6.8)	+4.2	−1.2
$CH_3CHOCH_3^+ +$ 2-Fpyridine	−7.1	−4.1	−4.6	+2.2[f]	−6.3
$c\text{-}C_3H_5COCH_3H^+ +$ oxazole	−4.3	+0.5	−4.6		
	−4.1	+1.1	−4.8		
	(−4.2)	(+0.8)	(−4.7)	0	+0.8
$c\text{-}C_3H_5COCH_3^+ +$ pyrrole	−5.1	−2.2	−3.8		
	−4.9	−1.6	−3.9		
	(−5.0)	(−1.9)	(−3.8)	+1.4	−3.4
$c\text{-}C_3H_5COCH_3H^+ + C_6H_5NH_2$	−4.7	+1.9	−5.8	+1.4[j]	+0.5[j]
				−2.2[f,k]	+4.1[f,k]
$CH_3CHOC_2H_5^+ +$ oxazole	−1.1	−1.8	−0.1	+2.2[e,f]	−4.0
$CH_3CHOC_2H_5^+ +$ 2F-pyridine	−3.6	−1.7	−2.5	+2.2[e,f]	−4.0
$oxazoleH^+ + C_6H_5NH_2$	−2.2	−2.2	−0.9	+1.4[j]	−3.6[j]
				−2.2[f,k]	0.0[f,k]
$oxazoleH^+ +$ 2-Fpyridine	−2.1	−0.1	−2.2	0	−0.1
$pyrroleH^+ +$ oxazole	−0.1	+1.0	−0.8	−1.4	+2.4
$pyrroleH^+ +$ 2-Fpyridine	−2.1	+0.6	−2.5	−1.4	+2.0
$C_6H_5NH_2H^+ +$ 2-Fpyridine	−0.1	+2.0	−1.3		
	−1.0	−0.2	−0.8		
	(−0.5)	(+0.9)	(−1.1)	−1.4[j]	+2.3[j]
				−2.2[f,k]	1.3[f,k]
$2\text{-}FpyridineH^+ + CH_2C(CH_3)OCH_3$	−2.4	+2.7	−3.9	−2.2[e,f]	+5.7
$2\text{-}FpyridineH^+ + CH_3NH_2$	−4.4	−5.7	−0.9		
	−4.3	−4.7	−1.5		
	−3.0	−1.2	−2.3		
	(−3.9)	(−3.9)	(−1.6)	−2.2[f]	−1.7
$2\text{-}FpyridineH^+ +$ thiazole	−4.5	NA[l]	NA[l]	0	−2.3
$CH_3C(CH_3)OCH_3^+ + CH_3NH_2$	−1.6	−5.7		0[e,f]	−5.7
$CH_3C(CH_3)OCH_3^+ +$ 3-Fpyridine	−2.0	−2.5		+2.2[e,f]	−4.7
$CH_3C(CH_3)OCH_3^+ + C_2H_5NH_2$	−5.5	−7.4		0[e,f]	−7.4
$CH_3NH_3^+ +$ thiazole	−1.5	NA[l]	NA[l]		
$CH_3NH_3^+ +$ 3-Fpyridine	−1.1	+3.0	−2.9	+2.2[f]	+0.8
$thiazoleH^+ +$ 3-Fpyridine	−0.4	NA[l]	NA[l]		
$thiazoleH^+ + i\text{-}C_3H_7NH_2$	−6.7	NA[l]	NA[l]		
$3\text{-}FpyridineH^+ + C_2H_5NH_2$	−2.4	−1.6	−1.4	−2.2[f]	+0.6
$3\text{-}FpyridineH^+ + i\text{-}C_3H_7NH_2$	−6.2	−3.2	−4.3	−2.2[f]	−1.0
$C_2H_5NH_3^+ + i\text{-}C_3H_7NH_2$	−3.2	+0.1	−3.3		
	−2.6	+0.6	−3.0		
	(−2.9)	(+0.4)	(−3.1)	0	−0.4
$C_2H_5NH_3^+ +$ pyridine	−3.8	−3.1	−5.7	+2.2[f]	−5.3
$C_2H_5NH_3^+ + t\text{-}C_4H_9NH_2$	−6.8	−0.5	−6.4		
	−5.5	+1.5	−6.5		
	(−6.2)	(+0.5)	(−6.5)	−2.2	+2.7
$i\text{-}C_3H_7NH_3^+ +$ azulene	−0.1	+3.8	−2.4	+2.2[f]	+1.6
$i\text{-}C_3H_7NH_3^+ +$ pyridine	−0.9	+2.5	−2.4		
	−2.0	+0.6	−2.4		
	−1.3	+2.7	−2.9		
	(−1.4)	(+1.8)	(−2.6)	+2.2[f]	−0.4
$i\text{-}C_3H_7NH_3^+ + (CH_3)_2NH$	−1.2	+1.2	−1.9	+0.8	+0.4
$i\text{-}C_3H_7NH_3^+ + t\text{-}C_4H_9NH_2$	−2.4	+2.0	−3.6	0	+2.0
$azuleneH^+ +$ pyridine	−1.0	−2.2	+0.3	0	−2.2
$azuleneH^+ + C_6H_5N(CH_3)_2$	−4.3	−3.9	−2.0	0	−3.9
$pyridineH^+ + (CH_3)_2NH$	−0.1	−1.8	+1.0		
	−0.2	−1.8	+0.9		
	(−0.2)	(−1.8)	(+1.0)	−1.4	−0.4
$pyridineH^+ + t\text{-}C_4H_9NH_2$	−1.3	−2.1	0.0		
	−1.2	−2.2	+0.1		
	(−1.3)	(−2.2)	(+0.1)	−4.4	+2.2
$pyridineH^+ + (CH_3)_3N$	−5.3	−0.9	−4.8	0	−0.9
$(CH_3)_2NH_2^+ + (CH_3)_3N$	−4.9	+1.2	−5.6	+1.4	−0.2

[a] $\Delta H°$ and $\Delta G°$ in kcal mol^{-1}, $\Delta S°$ in cal mol^{-1} K^{-1}. Average values from several measurements indicated in parentheses. [b] $\Delta G°_{600}$ calculated directly from the measured values of K_{600}, unless stated otherwise. [c] Calculated from $R \ln (\sigma(AH^+)\sigma(B))/(\sigma(BH^+)\sigma(A))$. [d] $\Delta S°_{structural} = \Delta S°_{experimental} - \Delta S°_{rot.\,sym}$. [e] Assuming nonplanar carbonium carbons in $(CH_3)_2CH^+$ and $(CH_3)_2COCH_3^+$ and a planar carbonium carbon in $(CH_3)_3CH^+$. Note that for $(CH_3)_2CCH_2 \rightarrow (CH_3)_3C^+$, $\Delta S°_{rot.\,sym} = R \ln (2/18) = -4.4$ cal/mol K (see also footnote *f*). [f] Using a symmetry term of $\Delta S°_{rot.\,sym} = -R \ln 3 = -2.2$ cal/mol K for the creation of a $-CH_3$ from $-CH_2$ and of $-NH_3$ from $-NH_2$ (ref 17). [g] Assuming protonation in the 4-position of C_6H_5F. [h] From extrapolation of the van't Hoff plot to 600 K. [i] Because of uncertainties in reactant concentrations, $\Delta G°$ and $\Delta S°$ were not determined. [j] Assuming protonation on the ring. [k] Assuming protonation on nitrogen.

Table II. Thermochemistry[a] of Association Reactions

	$-\Delta H°$		$-\Delta S°$		$\Delta H°_f$ (RXH$^+$)		PA(RX)	
	exp[b]	lit.[c]	exp[b]	lit.[d]	exp[e]	lit.[c]	exp.[f]	it.[c]
Condensation Reactions								
$C_3H_7^+ + HCN \rightarrow i\text{-}C_3H_7NCH^+$	39.6	37.0	45.2		183.4	186	208	206
$C_3H_7^+ + H_2S \rightarrow i\text{-}C_3H_7SH_2^+$	32.0	33.0	34.8		154.0	153	193.7	194.1
$t\text{-}C_4H_9^+ + NH_3 \rightarrow t\text{-}C_4H_9NH_3^+$	47.4		45.1					
	47.8		44.1					
	46.2		42.8					
	47.0		44.6					
	45.6		41.9					
	(46.8)	39.0	(43.7)	39.6	108.2	116	228.5	200.8
$NH_4^+ + i\text{-}C_4H_8 \rightarrow t\text{-}C_4H_9NH_3^+$	35.1		39.2					
	34.8		35.0					
	(35.0)	27.0	(37.1)	35.5	108	116	228.7	220.8
$t\text{-}C_4H_9^+ + (CH_3)_2S \rightarrow t\text{-}C_4H_9S(CH_3)_2^+$	44.2		42.6					
Clustering Reactions								
$NH_4^+ + NH_3$	26.9		29.2					
	24.8[g]		25.9[g]					
	27[h]		32[h]					
	25.4[i]		24.3[i]					
$CH_2CHCNH^+ + CH_2CHCN$	30.7		29.3					
$(CH_3)_2OH^+ + (CH_3)_2O$	32.1		31.0					
	31.9		31.7					
	(32.0)		(31.9)					
	29.5[j]		27.0[j]					
	30.7[k]		29.6[k]					
$(CH_3)_2COH^+ + (CH_3)_2CO$	30.7		28.2					
	30.1[l]		30.4[l]					
	29.6[m]		29.3[m]					
$C_6H_5COCH_3H^+ + C_6H_5COCH_3$	26.8		27.2					
$OH^- + H_2O$	26.8[n]							
	27.6[o]							
$CH_3O^- + CH_3OH$	29.3[n]							
	29.3[o]							

[a] $\Delta H°$ in kcal/mol, $\Delta S°$ in cal/mol K. [b] Present work unless indicated otherwise. [c] Calculated by using thermochemical data from ref 1. [d] Calculated by using $\Delta S°_{600}$ data from ref 15 and the following substitutions: $C_3H_7^+$ is approximated by the average $\Delta S°_{600}$ of C_3H_8 and $(CH_3)_2NH$, $t\text{-}C_4H_9^+$ by $i\text{-}C_4H_{10}$, $i\text{-}C_3H_7SH_2^+$ by $i\text{-}C_3H_7SH$, and $t\text{-}C_4H_7NH_3^+$ by $(t\text{-}C_4H_9NH_2 - R \ln 3)$ (for symmetry correction). [e] From present $\Delta H°$(condensation) and using $\Delta H°_f$ of the reactants from ref 1. [f] From present $\Delta H°_f$(RXH$^+$) and using $\Delta H°_f$ (RX) from ref 1. [g] Reference 27a. [h] Reference 27b. [i] Reference 28. [j] Reference 13. [k] Reference 29. [l] Reference 30. [m] Reference 31. [n] Reference 32. [o] Reference 11.

of protonation relative to a common reference compound as obtained from the thermochemistry, through the $\Delta H°$ and $\Delta G°$ ladders. However, this would include systematic errors that may build up through the ladders. The effects of these cumulative errors may be larger than the actual entropy changes. Therefore entropy effects are better evaluated from individual reactions.

5. Comparison with Thermochemical Ladders in the Literature. Long thermochemical ladders are subject to cumulative effects that are not readily noted in individual measurements. Therefore, comparing ladders from different sources is a useful way of identifying systematic differences between various techniques or laboratories. Several thermochemical ladders are plotted in Figure 15.

a. $\Delta G°$ Scales. Values of $\Delta G°$ from equilibrium measurements are obtained from eq 5 above. Cumulative differences between various ladders can arise from the ln K values or the assigned temperature.

The measured ln K values are obtained from ion intensity relations, where the intensities of AH^+ and BH^+ are usually different. Errors could occur if the detected signals are not proportional to the actual ion concentrations. However, the error would be systematic only if the intensities are correlated with proton affinities; for example, if the reactant with the higher PA has the larger ion signal in each equilibrium. This is not always the case.

Given a ladder of ln K values, the $\Delta G°$ values are scaled by the assigned temperature according to the relation $\Delta G° = RT \ln K$. A systematic expansion or contraction of the scale can occur if the assigned temperature is different from the actual temperature of the ion source. This is the most likely origin of systematic errors.

In the present study as well as those Lau and Kebarle[18,19] values of ln K were measured under well-thermalized high-pressure conditions and scaled by using the nominal temperature of 600 K. In Taft's low-pressure ICR work the ln K values were scaled by using 320 K. Figure 14 shows that the ICR $\Delta G°$ would agree with the present $\Delta G°$ scale if the ICR temperature was about 360 K.

The high-pressure $\Delta G°_{600}$ scale by Lau and Kebarle[18,19] is compressed by 4.4 kcal/mol over the 40 kcal/mol range from C_6H_6 to pyridine, and Figure 15 shows that an earlier $\Delta G°$ scale by Yamdagni and Kebarle is somewhat further compressed, compared with the present study. The 11% difference between the present ladder and that of Lau and Kebarle would correspond to a difference in temperature assignment of 66 K around 600 K. Given the calibrations described above, such a deviation in our source is unlikely. As to the temperature in Kebarle's early source, measurements on the $H_3O^+ \cdot H_2O$ dimer from that source differ from recent results by Hiraoka,[30] in a way that could correspond

(22) Meot-Ner (Mautner), M.; Sieck, L. W. *J. Phys. Chem.* **1990**, *94*, 7730.
(23) Karpas, Z.; Meot-Ner (Mautner), M. *J. Phys. Chem.* **1989**, *93*, 1859.
(24) Meot-Ner (Maunter), M. *J. Am. Chem. Soc.* **1991**, *113*, 862.
(25) Stone, J. A. In *Structure/Reactivity and Thermochemistry of Ions*; Ausloos, P., Lias, S. G., Eds.; Proceeding of NATO ASI Conference, Les Arcs. Reidl, 1986.
(26) Meot-Ner (Mautner), M.; Sieck, L. W. *Int. J. Mass Spectrom. Ion Processes* **1989**, *92*, 123.
(27) (a) Payzant, J. D.; Cunningham, A. J.; Kebarle, P. *Can. J. Chem.* **1973**, *51*, 3242. (b) Searles, S. K.; Kebarle, P. *J. Phys. Chem.* **1968**, *72*, 742.
(28) Tang, I. N.; Castleman, A. W. *J. Chem. Phys.* **1975**, *62*, 4756.
(29) Grimsrud, E. P.; Kebarle, P. *J. Am. Chem. Soc.* **1973**, *95*, 7939.

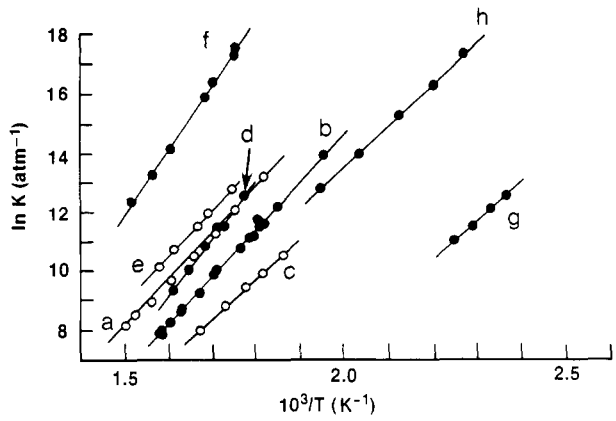

Figure 12. van't Hoff plots for equilibria for association reactions between the reactants: a. $(CH_3)_2OH^+ + (CH_3)_2O$; b. $i\text{-}C_3H_7^+ + H_2S$; c. $NH_4^+ + NH_3$; d. $i\text{-}C_3H_7^+ + HCN$; e. $(CH_3)_2COH^+ + (CH_3)_2CO$; f. $t\text{-}C_4H_9^+ + (CH_3)_2S$; g. $i\text{-}C_3H_7^+ + H_2O$; and h. $C_6H_5COCH_3H^+ + C_6H_5COCH_3$.

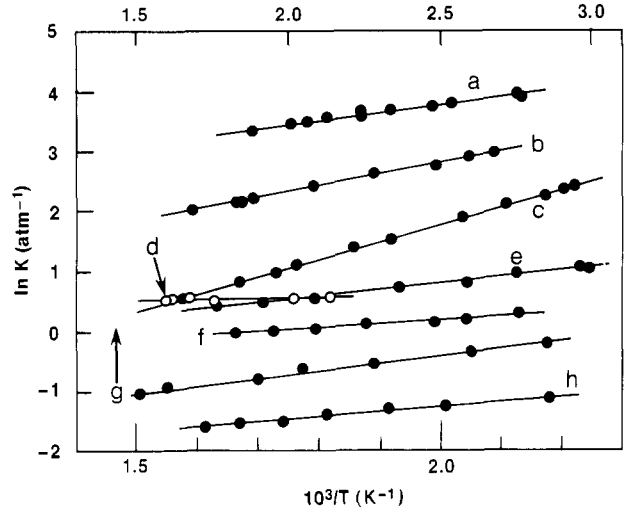

Figure 13. van't Hoff plots for proton-transfer equilibria between the reactants: a. 2-FpyridineH$^+$ + 2-methoxypropene; b. $CH_3CHOC_2H_5^+$ + 2-Fpyridine; c. 2-methoxypropeneH$^+$ + $C_2H_5NH_2$; d. $CH_3OH_2^+ + C_6H_5F$; e. 2-methoxypropeneH$^+$ + 3-Fpyridine; f. $CH_3CHOC_2H_5^+$ + oxazole; g. $C_6H_7^+ + C_6H_5F$ (upper scale); and h. 2-methoxypropeneH$^+$ + CH_3NH_2.

to a 10% deviation from the nominal temperature in Kebarle's early ion source at 600 K. This could be a possible explanation for the apparent compression in Kebarle's $\Delta G°$ scale. However, our results for association reactions agree well with Kebarle's (Table II), which suggests that the temperature scales in the two sources are not significantly different.

b. Comparison of the $\Delta H°$ Scale with Tabulated PA Values. The present ladder is the first directly measured $\Delta H°$ scale to cover key compounds over a large PA range. In the absence of such scales, comparisons can be made only with the evaluated PA tabulation of ref 1, except for the recent measurements of McMahon et al. which confirmed part of the present results.[21]

Below $i\text{-}C_4H_8$ the assigned relative PA values in ref 1 are derived mostly from $\Delta G°$ measurements but anchored to protonation energies from threshold and spectroscopic values. This portion of the tabulated scales therefore constitutes effectively a PA, i.e., $\Delta H°$ scale. Above $i\text{-}C_4H_8$, the tabulated values are also derived mostly from $\Delta G°$ determinations and assumed $I\Delta S°$ terms but not anchored to independent energy measurements. Therefore in this range the tabulated values in ref 1 constitute effectively a gas-phase basicity, i.e., a $\Delta G°$ scale, rather than relative proton affinities.

The present results are consistent with these considerations. Below $i\text{-}C_4H_8$ our $\Delta H°$ scale agrees with the tabulated PA values within 1 kcal/mol. On the bottom of the scale, CH_3OH and C_3H_6 agree with the tabulated values[1] within a fraction of a kcal/mol. Our measurements give a difference of 16.7 kcal/mol between the PAs of C_3H_6 and $i\text{-}C_4H_8$, in excellent agreement with the tabulated selected values from threshold measurements, 16.4 ± 2 kcal/mol. In contrast, above $i\text{-}C_4H_8$ our PAs are significantly different from the tabulated values.

The difference increases gradually with increasing PAs. Particularly notable is the present PA value for ammonia, 208.3 kcal/mol. Values for the proton affinity of ammonia have varied between 202 and 208 kcal/mol for decades, and the present result is close to the upper end. We note that $\Delta H°$ values obtained from the slopes of van't Hoff plots do not depend on the absolute concentration of NH_3, and this removes a difficulty associated with obtaining the PA from single-temperature equilibrium measurements. The difference between the PAs of $i\text{-}C_4H_8$ and NH_3 was measured directly as 12.8 ± 0.8 kcal/mol, an average value from six replicate measurements, and a similar value of 12.0 kcal/mol was confirmed recently by McMahon et al.[21] van't Hoff plots and further aspects of the $i\text{-}C_4H_8/NH_3$ system are given elsewhere.[22] Bridging through CH_3SCH_3, $CH_3COOC_2H_5$, $(C_2H_5)_2CO$, and $CF_3CH_2NH_2$ gave the PA difference as 12.3, 13.2, 12.6, and 11.2 kcal/mol, respectively (Figure 14), or an average of 12.3 kcal/mol. The $\Delta H°$ and $\Delta S°$ values for compounds bridging $i\text{-}C_4H_8$ and NH_3, namely $(CH_3)_2CO$, CH_3COOCH_3, $CH_3COOC_2H_5$, and $(C_2H_5)_2CO$ were also confirmed recently by McMahon et al.[21]

The direct and bridged measurements together give an average PA difference of 12.5 ± 0.7 kcal/mol at 600 K, which would give $PA(NH_3)$ = 208.4 kcal/mol. As we noted, extrapolation to 300 K may decrease the result by about 1 kcal/mol, and an uncertainty of ±1.5 kcal/mol in the absolute PA of $i\text{-}C_4H_8$ should be also considered. This would give $PA(NH_3)$ = 207.4 ± 1.6 kcal/mol at 300 K. This may be compared with the current tabulated value of 204 ± 3 kcal/mol.[1]

6. Condensation Reactions. In the ammonia/isobutene system the association equilibria (7) and (8) are observed simultaneously with the proton transfer equilibria.

$$t\text{-}C_4H_9^+ + NH_3 \rightarrow t\text{-}C_4H_9NH_3^+ \quad (7)$$

$$NH_4^+ + i\text{-}C_4H_8 \rightarrow t\text{-}C_4H_9NH_3^+ \quad (8)$$

The thermochemistry is given in Table II. The measured $\Delta H°_7$ = −46.8 ± 0.8 kcal/mol yields $PA(t\text{-}C_4H_9NH_2)$ as 228.7 kcal/mol, in excellent agreement with the proton affinity ladder that yields 229.2 kcal/mol. Similar results were obtained from reaction 8 measured in the same reaction systems. Note that the measurements were done at 600–680 K, but enthalpies in Table II were calculated by using 300 K values for the heats of formation of the reactants.[1] Corrections due to c_p effects may eventually be necessary. The measured large entropy changes of $\Delta S°_7$ = −43.7 ± 1.2 cal/mol K and $\Delta S°_8$ = −37.1 cal/mol K are consistent with covalent association, although somewhat more negative than expected (Table II). These results were also confirmed by McMahon et al.,[21] who measured $\Delta H°$ = −45.3 kcal/mol and $\Delta S°$ = −45.1 cal/mol K for the association of $t\text{-}C_4H_9^+$ with NH_3 (reaction 7).

The condensation thermochemistry can be entered into the PA ladder by linking the condensation reactant and product ions as illustrated in eqs 9 and 10.

$$t\text{-}C_4H_9^+ + t\text{-}C_4H_9NH_2 \rightarrow t\text{-}C_4H_9NH_3^+ + i\text{-}C_4H_8 \quad (9)$$

$$\Delta H°_9 = \Delta H°_7 + \Delta H°_f(NH_3) + \Delta H°_f(i\text{-}C_4H_8) - \Delta H°_f(t\text{-}C_4H_9NH_2) \quad (10)$$

It is important to note that to convert the association thermochemistry to PA differences as in eq 10, the heats of formation of three neutrals must be used, and uncertainties in these values affect the calculated values for $\Delta H°_9$. In contrast, direct proton affinity difference measurements do not require knowledge of $\Delta H°_f$ of the neutrals. Except for this increased uncertainty, condensation

(30) Lau, Y. K.; Saluja, P. P. S.; Kebarle, P. *J. Am. Chem. Soc.* **1980**, *102*, 7429.

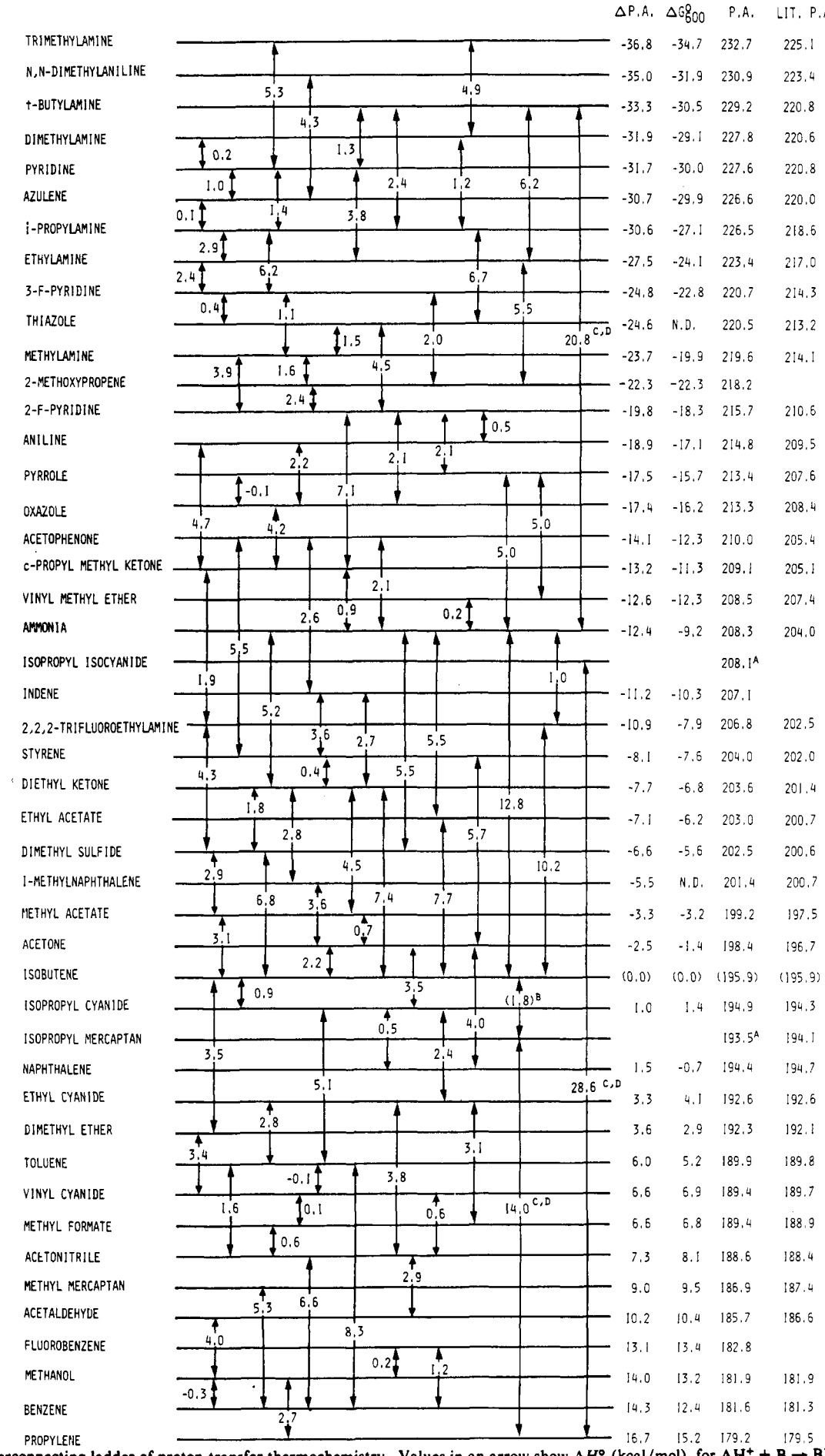

Figure 14. Interconnecting ladder of proton-transfer thermochemistry. Values in an arrow show $\Delta H°$ (kcal/mol), for $AH^+ + B \rightarrow BH^+ + A$, where A and B are the top and bottom compounds connected by the arrow: (a) from ref 1, (b) from ICR values, ref 1, (c) not included in the evaluated network and (d) from condensation equilibria.

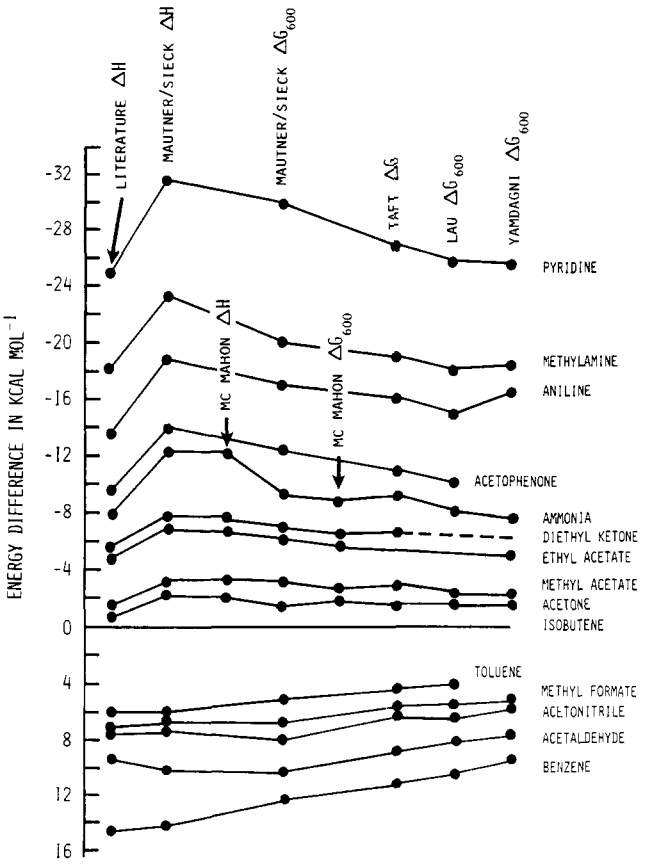

Figure 15. Thermochemical scales for proton affinities and gas-phase basicities. The data of Yamdagni from ref 3, Lau from ref 13, Taft as quoted in ref 1 and from personal communications, McMahon from ref 16, literature values from ref 1, and Mautner and Sieck from this work.

reactions bridge a large range in the PA ladder by a single measurement, as shown in Figure 14. In general, the error in one association measurement is comparable to or smaller than the cumulative error in a long ladder. In particular, reaction 7 connects in one step a primary standard to a PA range where no primary standards are otherwise available.

It is difficult to tie the reference ion i-$C_3H_7^+$ into the proton affinity ladder through proton-transfer equilibria, because of the reactivity of i-$C_3H_7^+$ with C_3H_6. Fortunately, the ion can also be generated without the presence of C_3H_6, by using a few percent C_3H_8 in CH_4. Under these conditions we measured the condensation equilibria of i-$C_3H_7^+$ with H_2S and HCN. The thermochemistry is shown in Table II.

In order to link the product ions of the condensation reactions into the PA ladder, the product ions must be connected also to reference compounds through proton-transfer equilibria. For i-$C_3H_7SH_2^+$ this was not possible because the ion decomposes at high temperatures, while clustering involving the reference compounds occurs at low temperatures. Therefore, we use the tabulated[1] PA from ICR measurements to link the product i-$C_3H_7SH_2^+$ with i-C_4H_8. The result gives a ΔPA between C_3H_6 and i-C_4H_8 of 15.8 kcal/mol, in good agreement with the tabulated value of 16.4 kcal/mol.

For i-$C_3H_7^+$ + HCN, the product ion i-$C_3H_7NCH^+$ can be linked to NH_3 by using the published ICR bracketing result for PA(i-C_3H_7NC), combined with the tabulated PAs for the bracketing reference compounds. The results give the PA difference between C_3H_6 and NH_3 as 27.6 kcal/mol, compared with 29.1 kcal/mol from the ladder. Using the same condensation result and ICR bracketing results and the selected value of PA(C_3H_6) = 179.5 kcal/mol gives PA(NH_3) = 207.1 kcal/mol, in good agreement with the value from the ladder, 208.3 kcal/mol. However, an uncertainty in the thermochemistry is that $\Delta H°_f$(i-C_3H_7NC) is not well-established.

7. Miscellaneous Reactions at High Temperatures. At high temperatures, usually above 600 K, we found new reactions in several systems. These reactions limit the temperature range of the proton-transfer equilibrium studies, but they provide information about ion chemistry at high temperatures. These observations illustrate some of the limitations of the equilibrium method and will be discussed here briefly.

a. Thermally Activated Condensation. In acetaldehyde, condensation reaction 11, possibly aldol condensation to yield protonated crotonaldehyde, became significant above 620 K.

$$CH_3CHOH^+ + CH_3CHO \rightarrow CH_2CHC(CH_3)OH^+ + H_2O \quad (11)$$

In protonated sulfur compounds such as $CH_3SH_2^+$, clustering is weak, and this should facilitate proton-transfer equilibrium measurements. However, we observed that the condensation reaction 12 becomes important above 500 K.

$$CH_3SH_2^+ + CH_3SH \rightarrow (CH_3)_2SH^+ + H_2S \quad (12)$$

Analogous reactions occur in alcohols, and we observed recently that the slow rate constants ($1-5 \times 10^{-10}$ cm^3 s^{-1}) have no significant temperature coefficients.[23] In contrast, the reaction in the sulfur compound showed a significant temperature coefficient, and this prevented proton-transfer equilibrium studies at high temperatures. On the other hand, below 450 K we observed another apparent condensation product, $CH_3SSCH_3H^+$, which also limited proton-transfer studies at low temperatures.

Addition reactions other than activated condensation usually decrease with increasing temperature but can still be significant at high temperatures in some cases. We observed the association of carbonium ions with sulfur compounds even above 600 K. For example, such an adduct was observed between t-$C_4H_9^+$ and $(CH_3)_2S$. A temperature study yielded the data in Table II which is the first thermochemical data for a tertiary sulfonium ion, namely $(CH_3)_2S$-t-$C_4H_9^+$.

b. Slow Proton-Transfer Reactions. The rate constants of most of the proton-transfer reactions were about the expected collision rate, $1-2 \times 10^{-9}$ cm^3 s^{-1}. However, some proton-transfer reactions were significantly slower, sometimes with negative temperature coefficients. One such case was *N*,*N*-dimethylanilineH$^+$ + azulene, where k decreased from 2×10^{-9} at 400 K to 0.2×10^{-9} cm^3 s^{-1} at 600 K. The steric hindrance at the dimethylaniline nitrogen center may be responsible, analogous to slow proton transfer with negative temperature coefficients in hindered alkylpyridines.[24] Proton transfer is also slow between t-$C_4H_9^+$ and naphthalene ($k_{500} = 0.2 \times 10^{-10}$ cm^3 s^{-1}), furanH$^+$ and naphthalene ($k_{600} = 0.8 \times 10^{-10}$ cm^3 s^{-1}), and furanH$^+$ and toluene ($k_{500} = 0.2 \times 10^{-10}$ cm^3 s^{-1}). These reactions involve proton transfer between carbonium ions and an aromatic carbon base, and the slow rates are similar to those observed in proton transfer between alkylbenzenes.[25]

c. Thermal Rearrangements. In the context of the present study attempts were made to measure the PA of cyclooctatetraene. Measurements against $(C_2H_5)_2CO$, $C_6H_5COCH_3$, aniline, and 2-Fpyridine showed apparent equilibria, but the apparent gas-phase basicity increased strongly with decreasing temperature and the apparent $\Delta S°$ values were unreasonable. For example, for $C_6H_5COCH_3H^+$ + cyclooctatetraene, the apparent results were $\Delta H° = -6.4$ kcal/mol and $\Delta S° = -16.8$ cal/mol K. The results may reflect an artifact caused by the rearrangement of the neutral or protonated cyclooctatetraene at high temperatures to styrene, giving an apparent PA close to that compound. Similarly, problems were observed with furan, suggesting possible ring opening at high temperatures.

d. Thermal Decompositions. In addition to the above processes, many of the present complex organic ions may decompose at significant rates above 600 K. For example, we observed that $C_2H_5OH_2^+$ forms H_3O^+ + C_2H_4[26] and i-$C_3H_7OH_2^+$ and i-$C_3H_7SH_2^+$ form $C_3H_7^+$. Such decompositions can lead to deviations from the van't Hoff plots above 600–650 K. Similar observations suggested that $HCONH_2$ or $HCONH_2H^+$ decompose above 600 K.

In summary, ion chemistry at high temperatures, usually above

600 K, shows a variety of new kinetic features and reaction channels. These create problems for thermochemical measurements but also offer an interesting field of study.

Conclusions

A ladder of relative proton affinities was obtained from variable-temperature proton-transfer equilibria. The measurements span over 50 kcal/mol in $\Delta H°$ and $\Delta G°$. The accuracy of the measurements was verified by constructing analogous ionization energy and acidity scales involving known absolute reference standards. The accuracy was also tested by comparing the $\Delta H°$ and $\Delta G°$ scales, where the sources of error are different. These tests suggest that thermochemical ladders from variable-temperature pulsed high-pressure measurements can span an energy range of 50 kcal/mol with an accuracy of ±2 kcal/mol. Reproducibility and the consistency of cycles in the ladder suggest that the $\Delta H°$ values for individual reactions are accurate to ±0.5 kcal/mol and the assigned proton affinities are accurate to ±1 kcal/mol.

Our proton affinities below i-C_4H_8 agree well with literature values that were tied to known reference standards.[1] Above i-C_4H_8, where no such standards are available, the present measurements yield proton affinities up to 8 kcal/mol higher than the literature values.[1] The present values are supported by condensation equilibria which link in one step a wide range of the PA scale. Some of the present results were also confirmed by recent measurements by McMahon et al., by using a pulsed high-pressure mass spectrometer with a significantly different design.[21] We also note that Bisling et al.,[33] as a result of photoionization studies of hydrogen-bonded neutral clusters, derived proton affinities for simple alkylamines which are in good agreement with our values. A further test may be provided by using vinyl ethers as absolute standards, when accurate calorimetric and appearance potential data become available.

In order to derive 0 or 300 K proton affinities from the present measurements, heat capacity data on the ions is necessary. Estimates of c_p from analogous neutrals suggest that these corrections would be at most 1 kcal/mol.

The present $\Delta S°$ values test the frequent assumption that entropy changes in proton-transfer equilibria can be accounted for by rotational symmetry changes. This assumption is verified in most of the present systems, although additional structural entropy changes up to 6 cal/mol K occur in several classes of compounds such as aromatics and olefins. For aromatics, the entropies do not indicate any major effects due to a dynamic proton, as were observed in some halotoluenes. These findings agree with the observations of Stone, who also did not find any unexpectedly large entropy effect in the protonation of alkylbenzenes,[20] and also with the arguments of Jennings et al., who do not expect such behavior in unsubstituted aromatics.[7] Our results also confirm that the protonation of olefins involves small overall entropy change 0–2 cal/mol K, possibly due to compensating effects of rotational entropy and internal rotational symmetry changes.

The present work is the first to examine a large portion of the proton affinity scale by direct $\Delta H°$ measurements. Such measurements are laborious and subject to limitations because of a rich ion chemistry at high temperatures and clustering at low temperatures. However, the results demonstrate that direct $\Delta H°$ determinations are necessary when no absolute local reference standards are available for portions of a thermochemical ladder.

Acknowledgment. This work was supported by a grant from the Division of Chemical Sciences, Office of Basic Energy Sciences, U.S. Department of Energy. We thank Drs. S. G. Lias, P. Ausloos for critical review, Dr. J. F. Liebman for helpful comments, Dr. R. Goldberg for help with calculations using the NIST Thermochemical Network Program, and Dr. T. B. McMahon for making available his results prior to publication.

(31) Hiraoka, K.; Takimoto, H. *J. Phys. Chem.* **1986**, *90*, 5910.
(32) Meot-Ner (Mautner), M.; Sieck, L. W. *J. Phys. Chem.* **1986**, *90*, 5910.
(33) Bisling, P. G. E.; Ruhl, E.; Brutschy, B.; Baumgartel, H. *J. Phys. Chem.* **1987**, *91*, 4310.